

Free Energies of Hydration in the Gas Phase of the Anions of Some Oxo Acids of C, N, S, P, Cl, and I

Arthur T. Blades, John S. Klassen, and Paul Kebarle*

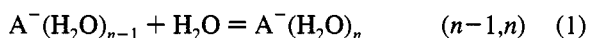
Contribution from the Department of Chemistry, University of Alberta,
Edmonton, Alberta, Canada T6G 2G2

Received June 2, 1995[Ⓢ]

Abstract: Hydration equilibria: $A^{z-}(H_2O)_{n-1} + H_2O = A^{z-}(H_2O)_n$, where $z = 1, 2$, were determined involving ions A^{z-} produced by electrospray. An ion source operating at 10 Torr pressure with which thermal conditions can be achieved was used, and the ions were sampled by means of an orifice leading to a mass spectrometer. Free energy values, $\Delta G_{n-1,n}^\circ$, were obtained at 293 K for 16 carboxylic acid anions, RCO_2^- , and for a total of 17 monoanions of the oxo acids of N, P, S, Cl, and I. The $-\Delta G_{0,1}^\circ$ values for the above lead to an approximate linear relationship with the gas phase acidities, $\Delta G_{ac}^\circ(AH)$, corresponding to the dissociation, $AH = A^- + H^+$. Therefore, the magnitudes of the $\Delta G_{0,1}^\circ$ values can be interpreted on the basis of the well understood factors which determine gas phase acidities. Determinations of $\Delta G_{n-1,n}^\circ$ for dicarboxylates: $HCO_2(CH_2)_kCO_2^-$ where $k = 0$ to 8, were also obtained. The hydration exoergicities of these compounds are much lower than those of the RCO_2^- anions where R = alkyl. The weaker hydration of the dicarboxylates is due to stabilization of these anions by intramolecular hydrogen bonding which leads to cyclization. Anions where k is low have higher hydration exoergicities, because these anions are less stabilized by the internal H bond which is strained for these species. Hydration free energies for the doubly charged A^{2-} anions, $CO_2(CH_2)_kCO_2^{2-}$, and oxo anions: SO_4^{2-} , SeO_4^{2-} , $S_2O_3^{2-}$ (thiosulfate), $O_3SSO_3^{2-}$ (dithionate), $O_3SC_2H_4SO_3^{2-}$, $O_3SOOSO_3^{2-}$ (persulfate), $O_3SS_2SO_3^{2-}$ (tetrathionate), and 1,5-naphthalene disulfonate were also obtained. The factors affecting the hydration exoergicities of these compounds are discussed.

Introduction

Determinations of gas phase equilibria involving singly charged ions and solvent molecules such as H_2O (see eq 1), or other ligands, were initiated some 30 years ago.^{1,2}



The sequential bond free energies, $\Delta G_{n-1,n}^\circ$, and enthalpies, $\Delta H_{n-1,n}^\circ$, resulting from such equilibrium measurements have provided a wealth of data^{2,3} on ion–solvent and ion–ligand interactions for positive M^+ and negative A^- ions.

Many ions of great interest in condensed phase chemistry and biochemistry could not be produced in the gas phase by the conventional methods.^{1–3} For example, negative ions A^- are obtained by deprotonation of AH in the gas phase, but this method requires that the AH compounds be sufficiently volatile. Multiply charged ion–ligand L complexes such as $M^{2+}L_n$ and $A^{2-}L_n$ are also very difficult, if not impossible, to produce in the gas phase by conventional methods.

Electrospray mass spectrometry (ESMS) developed by John Fenn and co-workers⁴ is a method with which electrolyte ions present in solution can be transferred to the gas phase.⁵ With ES it is possible to obtain gas phase singly or multiply charged ion–ligand complexes,⁶ multiply protonated peptides and

proteins,⁷ doubly charged anions⁸ such as SO_4^{2-} and HPO_4^{2-} and multiply deprotonated nucleic acids.⁹ While the major impact of ESMS is in bioanalytical mass spectrometry, the method can be also of great value for physicochemical measurements.

Recently, we described^{10,11} an ion source–reaction chamber with which ion–molecule equilibria involving ES produced ions can be determined. The first experiments^{10,11} involved positive ions. The present work provides data from our first equilibrium determinations involving negative ions.

Free energy values, $\Delta G_{n-1,n}^\circ$, for the hydration equilibria, eq 1, involving some 40 singly charged anions A^- and 15 doubly charged anions A^{2-} were obtained in the present work. The acids from which the anions formally derive are oxo acids of carbon, nitrogen, phosphorus, sulfur, chlorine, and iodine. In spite of the great variety of anions, a systemization and rationalization of the results can be achieved for both the singly and doubly charged anions, as will be shown in the Discussion.

Experimental Section

A detailed account of the apparatus and method was given elsewhere.¹¹ Here we provide only a brief description of the essential features. The electrospray generator and the ion source–reaction chamber are shown in Figure 1. The solution consisting of methanol solvent and 10^{-4} mol/L of the sodium or potassium salt, MA or M_2A , of a monobasic or dibasic anion is passed in slow flow, $\sim 2 \mu\text{L}/\text{min}$, through the electrospray capillary, ESC. The tip of the ESC, 0.7 mm o.d., 0.4 mm i.d., is of stainless steel and is at a high negative potential.

(7) Bruins, A. P.; Covey, T. R.; Henion, J. D. *Anal. Chem.* **1987**, *59*, 2642.

(8) Blades, A. T.; Kebarle, P. *J. Am. Chem. Soc.* **1994**, *116*, 10761.

(9) (a) Limbach, P. A.; Crain, P. F.; McCloskey, J. A. *J. Am. Soc. Mass Spectrom.* **1995**, *6*, 27. (b) Smith, R. D.; Lou, J. A.; Edonds, C. G.; Barinaga, C. J.; Udseth, H. R. *Anal. Chem.* **1990**, *62*, 882.

(10) Klassen, J. S.; Blades, A. T.; Kebarle, P. *J. Am. Chem. Soc.* **1994**, *116*, 12075.

(11) Klassen, J. S.; Blades, A. T.; Kebarle, P. *J. Phys. Chem.* In press.

[Ⓢ] Abstract published in *Advance ACS Abstracts*, October 15, 1995.

(1) Hogg, A. M.; Haynes, R. N.; Kebarle, P. *J. Am. Chem. Soc.* **1966**, *88*, 28.

(2) Kebarle, P. *Annu. Rev. Phys. Chem.* **1977**, *28*, 455.

(3) Keese, R. G.; Castleman, A. W. *J. Phys. Chem. Ref. Data* **1986**, *15*, 1011.

(4) Yamashita, M.; Fenn, J. B. *J. Phys. Chem.* **1984**, *88*, 4451. Fenn, J. B.; Mann, M.; Meng, C. K.; Wong, S. F.; Whitehouse, C. M. *Science* **1985**, *246*, 64.

(5) Kebarle, P.; Tang, L. *Anal. Chem.* **1993**, *65*, 272A.

(6) Blades, A. T.; Jayaweera, P.; Ikonou, M. G.; Kebarle, P. *J. Chem. Phys.* **1990**, *92*, 2900. Blades, A. T.; Jayaweera, P.; Ikonou, M. G.; Kebarle, P. *Int. J. Mass Spectrom. Ion Processes* **1990**, *102*, 251.

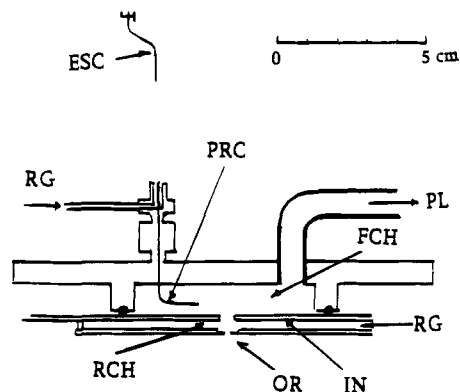


Figure 1. Electrospray ion source and reaction chamber: ESC, electro-spray capillary at high negative potential which emits spray of negatively charged droplets into atmosphere. Droplets lead ultimately to negative gas phase ions which are drawn against a flow of N_2 source gas, SG, into the forechamber, FCH, through the pressure reducing capillary, PRC. Forechamber, FCH, is maintained at about 10 Torr via the pumping lead, PL. Gas jet and ions escape from PRC into forechamber, FCH. Ions are deflected by electric field into reaction chamber, RCH, also at 10 Torr. Reagent gas, RG, mixture is supplied to reaction chamber where ions reach hydration equilibria. Ions are sampled through orifice OR leading to vacuum of mass spectrometer.

A fine spray of small droplets, which are negatively charged due to an excess of negative electrolyte ions in them, is emitted from the capillary tip into the ambient air. Solvent evaporation from the droplets leads to droplet shrinkage and an increase of the charge to surface area ratio of the droplets. This destabilizes the droplets and leads to droplet fissions. Repeated fissions ultimately lead to gas phase ions.⁵

The spray containing the ions is sucked into the forechamber of the ion source, FCH, via the pressure reducing capillary, PRC. The forechamber, FCH, and the reaction chamber, RCH, are maintained at 10 Torr by outflow through pumping lead, PL. A gas jet containing the ions escapes from the capillary PRC. The ions are deflected out of the jet by an electric field applied between the forechamber, FCH, and the top plate, IN, of the reaction chamber, RCH. Some of the deflected ions drift into RCH through a 4 mm diameter orifice in IN. A reagent gas mixture consisting of 10 Torr N_2 bath gas and vapor $L = H_2O$ at a known partial pressure, generally between 1–70 m Torr, flows slowly through RCH, enters FCH, and is pumped out. The ions entering RCH are drifted across RCH toward the sampling orifice OR (100 μm) by a very weak electric field. The drift velocities are very low, and the internal energy of the ions remains thermal.¹¹ The ions react with the water molecules and reach equilibrium within their residence time of $\sim 100 \mu s$ in RCH.¹¹ Ions escaping through the orifice OR into the vacuum are detected with a quadrupole mass spectrometer.

Typical electrode potentials used were as follows: ESC -4.5 kV, SG exit tube -500 V, PRC and top of FCH -42 V, IN -17 V, OR plate -3 V, first electrode in vacuum, not shown in Figure 1, -0.5 V.

The equilibrium constants are determined from the mass spectrometrically measured intensities of the ions $A^-(H_2O)_n$ and $A^-(H_2O)_{n-1}$, whose ratio, I_n/I_{n-1} , is taken to be equal to the ion concentration ratio in RCH at equilibrium so that eq 2 can be applied.

$$K_{n-1,n} = \frac{I_n}{I_{n-1}P_{H_2O}} \quad (2)$$

Results and Discussion

a. Ion Abundances and $K_{n-1,n}$ Determinations in Some Typical Experiments. A mass spectrum giving the ion abundances at different mass to charge, m/z , ratios is shown in Figure 2. It was obtained from electrospray of a 5×10^{-5} mol/L solution of disodium suberate in methanol. The reagent gas used in the reaction chamber was 12 Torr N_2 and 5 mTorr H_2O . The suberate dianion, $CO_3^{2-}(CH_2)_6CO_3^{2-}$ under these conditions is observed as the $Sub^{2-}(H_2O)_n$ where the $n = 3$ hydrate is the

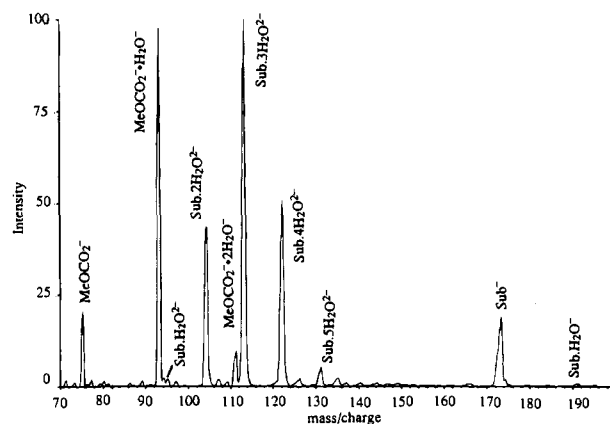


Figure 2. Ion intensities observed from a solution of $Na_2CO_3(CH_2)_6CO_3$, disodium suberate. Both the doubly, Sub^{2-} , and singly Sub^- charged ions are observed. A pressure of 7 mTorr in the reaction chamber, RCH, Figure 1, leads to the observed hydration of Sub^{2-} and Sub^- . The methoxycarbonate ion $MeOCO_2^-$ is due to a sodium bicarbonate impurity. This singly charged ion is much more strongly hydrated than Sub^- .

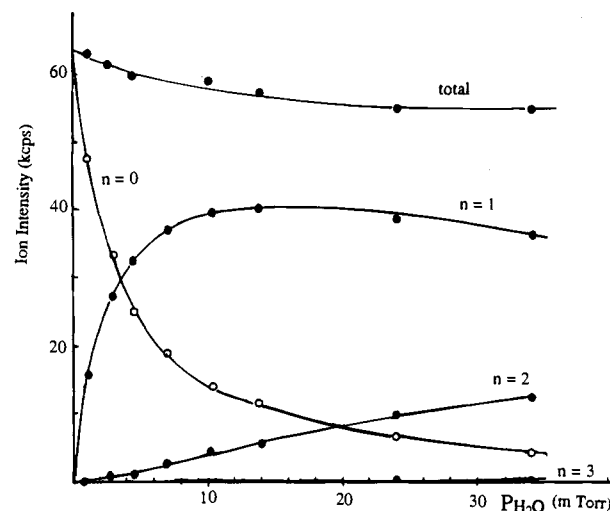


Figure 3. Ion intensities for $NO_3^-(H_2O)_n$ ions determined at different constant H_2O pressures in the reaction chamber. Actually observed ion intensities in kilocounts per second (kcps) are given, see vertical axis. The total intensity, which is approximately constant with H_2O pressure, is also given.

most abundant. The singly charged Sub^- which is also observed under the same conditions is essentially completely unhydrated. The methyl ester of the carbonic acid anion $MeOCO_2^-$ is often observed in electrospray with methanol as solvent.⁸ The $MeOCO_2^-$ is much more strongly hydrated than the singly charged Sub^- . The very different strength of hydration for Sub^{2-} , Sub^- , and $MeOCO_2^-$ observed in Figure 2 represents three different types of hydration interactions explored via the equilibrium determinations in the present work.

The dependence of the ion hydrate intensities on the partial pressure of H_2O is illustrated in Figure 3 for the nitrate ion NO_3^- . These data were obtained from determinations of the hydrate intensities at eight different H_2O partial pressures. The intensities shown in Figure 3 were used for the evaluation of the intensity ratio, I_n/I_{n-1} , plots, Figure 4. The ion intensities observed in Figure 3 are quite high except for the $NO_3^-(H_2O)_3$ ion. For a H_2O pressure of 7 mTorr, this ion had an intensity of only 20 counts/s. Intensities at this and higher levels can be measured quite accurately by time averaging and therefore all three equilibrium constants $K_{0,1}$, $K_{1,2}$, and $K_{2,3}$ could be determined from the data obtained. The total $NO_3^-(H_2O)_n$ ion

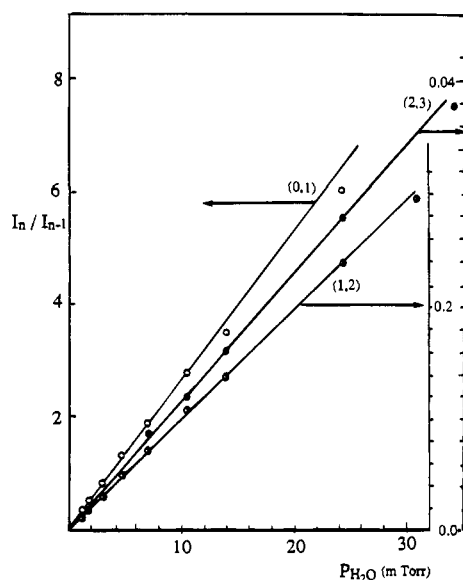


Figure 4. Plots of ion intensities ratio, I_n/I_{n-1} , corresponding to ion intensities $\text{NO}_3^-(\text{H}_2\text{O})_n$ and $\text{NO}_3^-(\text{H}_2\text{O})_{n-1}$, see Figure 3, versus partial pressure of H_2O , $P_{\text{H}_2\text{O}}$, in the reaction chamber. The slope of the straight line is used to evaluate the equilibrium constant: $I_n/I_{n-1} = K_{n-1,n}P_{\text{H}_2\text{O}}$. Values of $(n-1, n)$ are given with respective plots. Note that three different vertical scales were used to accommodate the widely differing I_n/I_{n-1} ratios.

intensity is also shown in Figure 3. Ideally, this intensity should have remained constant. A decrease with H_2O pressure is observed but the decrease is small.

The equilibrium constant plots, on the basis of eq 2, are shown in Figure 4. Good linear plots are observed for all three equilibria. In general, good straight line plots going through the origin were observed in all measurements.

b. Hydration of Singly Charged Anions. The hydration free energies $\Delta G_{n-1,n}^\circ$ for singly charged anions A^- are summarized in Table 1. Section (a) provides the data for the bicarbonate anion and a variety of carboxylic acids RCO_2^- , while section (b) deals with anions of some oxo acids of the N, P, S, Cl, and I atoms. The range of $(n-1, n)$ values provided for a given anion was dependent on the equilibria which could be determined at the experimental temperature $T = 293$ K and the range of H_2O pressures, ~ 1 to 70 m Torr, which led to good linear plots, see preceding section and Figures 3 and 4.

Previous determinations in the literature,^{3,12-17} mostly of $\Delta G_{0,1}^\circ$, with which the present results can be compared are available only for a few of the anions (CH_3CO_2^- , NO_2^- , NO_3^- , H_2PO_4^- , HOSO_3^-), see Table 1. In general, the present results do not differ by more than 0.3 kcal/mol from the literature results, and this may be considered as very good agreement. The literature data quoted for all anions except H_2PO_4^- are experimental results. The $\Delta G_{0,1}^\circ$ and $\Delta G_{1,2}^\circ$ given for H_2PO_4^- are based on recent high level ab initio calculations by Houk and co-workers.¹⁶ These authors do not list directly the above values since their calculations were made for a different purpose;

(12) Meot-Ner, (Mautner) M. *J. Am. Chem. Soc.* **1988**, *110*, 3854. Payzant, J. D.; Yamdagni, R.; Kebarle, P. *Can. J. Chem.* **1971**, *49*, 3308.

(13) Keesee, R. G.; Lee, N.; Castleman Jr., A. W. *J. Am. Chem. Soc.* **1979**, *101*, 2599.

(14) Davidson, J. A.; Fehsenfeld, F. C.; Howard, C. J. *Int. J. Chem. Kinet.* **1977**, *9*, 17.

(15) Keesee, R. G.; Castleman, Jr., A. W. *J. Am. Chem. Soc.* **1989**, *111*, 9015.

(16) Wu, Y. D.; Houk, K. N. *J. Am. Chem. Soc.* **1993**, *115*, 11997.

(17) Bohringer, H.; Fakey, D. W.; Fehsenfeld, F. C.; Ferguson, E. E. *J. Chem. Phys.* **1984**, *81*, 2805.

Table 1. Free Energies of Hydration of Anions A^- and of Acid Dissociation, $\Delta H = \text{A}^- + \text{H}^+$

ion	$-\Delta G_{n-1,n}^\circ$ (kcal/mol) ($n-1, n$)			$\Delta G_{\text{acid}}^\circ$ ^b (kcal/mol)
	0.1	1.2	2.3	
a. Carboxylates, RCO_2^-				
CH_3CO_2^-	9.4 (9.75) ^d	6.8	5.2	341.5
$\text{C}_2\text{H}_5\text{CO}_2^-$	9.3	6.6	5.1	340.3
HCO_2^-	9.2	6.8	5.1	338.2
$\text{CH}_3\text{OCH}_2\text{CO}_2^-$	8.6	6.1	4.8	
HOCO_2^-	(8.50) ^e	(6.2) ^e	(4.6) ^e	(334.0) ^c
$\text{CH}_3\text{OCO}_2^-$	8.3	6.1	4.6	(331.8) ^c
$\text{CH}_2\text{FCO}_2^-$	8.3	5.9	4.6	331.0
$\text{C}_6\text{H}_5\text{CO}_2^-$	8.1	5.7	4.5	331.7
$\text{CH}_2\text{ClCO}_2^-$	7.7			328.8
$\text{CH}_3\text{CHOHCO}_2^-$	7.7	5.3		(326.6) ^c
$\text{CHF}_2\text{CO}_2^-$	7.5	5.3		323.5
$\text{CH}_2\text{ICO}_2^-$	7.2	5.3	4.3	(322.6) ^c
$\text{CH}_2\text{CNCO}_2^-$	7.1	5.2		323.7
$\text{CHCl}_2\text{CO}_2^-$	6.8	4.9		321.9
CF_3CO_2^-	6.8	4.7		316.3
$\text{CCl}_3\text{CO}_2^-$	5.8			(309.6) ^c
b. Anions of Some Oxo Acids of N, P, S, Cl, and I				
NO_2^-	~ 8.5 (8.0-8.4) ^f	6.00	4.5	332.3 ± 4.5^g
NO_3^-	7.1 (6.7-7.1) ^f	5.2	3.9	$318.18^{g,h}$
H_2PO_4^-	8.4	6.4	4.7	
$(\text{HO})\text{HPO}_4^-$	7.8	6.6	5.2	
$(\text{HO})_2\text{PO}_4^-$	7.6 (7.5) ^m	6.1 (5.8) ^m	4.8	
PO_3^-	(6.27) ^l (6.20) ^m	(4.90) ^l (4.00) ^m		303.8^k
CH_3SO_3^-	6.9	5.4	4.4	315.00^i
$\text{C}_7\text{H}_{15}\text{SO}_3^-$	6.3	5.0		
$\text{C}_6\text{H}_5\text{SO}_3^-$	5.9	4.4		
$\text{C}_2\text{H}_5\text{OSO}_3^-$	5.8	4.6		
HOSO_3^-	5.9 (6.0) ⁿ	4.7		302.6^k
CF_3SO_3^-	4.6	3.8		$299.^k 299.^l$
ClO_2^-	9.0	6.1	4.8	
ClO_3^-	6.2	4.7		
ClO_4^-	4.8			
BrO_3^-	6.5	5.0		
IO_3^-	6.4	5.0	4.2	
IO_4^-	4.3			

^a Free energy change in kcal/mol, standard state 1 atm for hydration equilibria $(n-1, n)$: $\text{A}^-(\text{H}_2\text{O})_{n-1} + \text{H}_2\text{O} = \text{A}^-(\text{H}_2\text{O})_n$ at 293 K determination from this laboratory. Literature values in brackets. ^b Free energy change for reaction: $\text{HA} = \text{H}^+ + \text{A}^-$ in kcal/mol. Standard state 1 atm 298 K. Unless otherwise indicated values given are from Cunningham and Kebarle²⁰ or Caldwell, Renneboog, and Kebarle.²¹ ^c Estimated acidity value based on relationship with $\Delta G_{0,1}^\circ$, see Figure 4. ^d Meot-Ner.¹² ^e Castleman.¹³ ^f Castleman.³ ^g Lias.²⁵ ^h Fehsenfeld.¹⁴ ⁱ Taft.²² ^k Viggiano.²³ ^l Castleman.¹⁵ ^m Houk.¹⁶ ⁿ Fehsenfeld.¹⁷

however, total energies and entropies provided for the reactants of eq 1 allow an evaluation of the free energies quoted in Table 1.

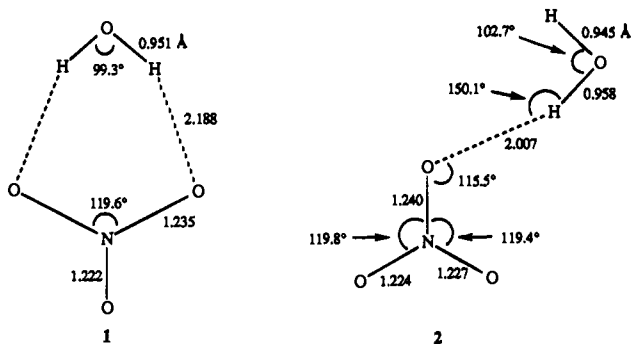
The anions listed in Table 1 represent a wide range of chemical types, and a concise examination of the relationship between the observed energies and the chemical properties of the anions appears challenging. Fortunately this is possible on the basis of a correlation between the hydration energy $\Delta G_{0,1}^\circ$ and the Arrhenius gas phase basicity of A^- . Previous experimental determinations^{18,19} have shown that the bond strength in hydrogen bonded complexes, $\text{XH} \cdots \text{A}^-$, increases with the gas phase acidity of XH and the gas phase basicity of A^- . The

(18) (a) Yamdagni, R.; Kebarle, P. *J. Am. Chem. Soc.* **1971**, *93*, 7139. (b) Payzant, J. D.; Yamdagni, R.; Kebarle, P. *Can. J. Chem.* **1971**, *49*, 3308. (c) Cumming, J. B.; French, J. B.; Kebarle, P. *J. Am. Chem. Soc.* **1977**, *99*, 6999. (d) Caldwell, G.; Kebarle, P. *Can. J. Chem.* **1985**, *63*, 1399. (e) Paul, G. J. C.; Kebarle, P. *Can. J. Chem.* **1990**, *68*, 2070.

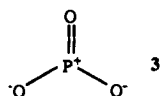
less than 1 kcal/mol while the relative $\Delta G_{0,1}^\circ$ values error is probably less than 0.3 kcal/mol. At present, it is not clear whether the observed large deviations are due to accidental, larger experimental errors or due to a special intrinsic difference in the energies of acid dissociation and anion hydration.

The trichloroacetate anion has the lowest $-\Delta G_{0,1}^\circ$ value among the carboxylates shown in Table 1. The value is lower by ~ 1 kcal/mol than the result for trifluoroacetate, and this indicates that trichloroacetic acid is considerably more acidic than the trifluoro compound. Previous acidity determinations for the di- and monosubstituted acids^{20,21} also have shown that the chlorosubstituted acids have higher gas phase acidities than the fluoro substituted analogues.

The correlation between acidities and hydration energies, Figure 5, is less good when oxo anions other than the carboxy anions are included. One might consider that this could be due to significantly different structures of the anion hydrates for the oxoanions of C, N, P, S etc. However, theoretical calculations for the *mono* hydrates of $(\text{HCO}_2^-)^{26}$ $(\text{NO}_3^-)^{27}$ $(\text{PO}_3^-)^{16,28}$ and $(\text{H}_2\text{PO}_4^-)^{16}$ predict the same doubly hydrogen-bonded structure. The structure is illustrated below for $\text{NO}_3^- \cdot \text{H}_2\text{O}$, based on Schaefer's²⁷ calculations, see structure 1. The singly hydrogen-bonded structure, 2, is less stable by ~ 2.2 kcal/mol.²⁷ Similar stability differences between the structures 1 and 2 are present for the other anions,^{16,26-28} and this means that differences of the H bonded structures are not likely to be responsible for relative scatter in the correlation, Figure 5. However, more subtle differences may be present. In a discussion of the bonding of H_2O to PO_3^- , Schaefer *et al.*²⁸ point out that changes in the bond distances of PO_3^- , namely a shortening of the P-O



bond not participating in the hydrogen bonding by ~ 0.008 Å on hydrate formation, structure 1, relative to the bond length in the free PO_3^- and a lengthening of the two P-O bonds by 0.003 Å, indicates an increased contribution of the Lewis-type structure 3 in the hydrate relative to that in the free PO_3^- . Electronic charge redistributions of this type favoring the doubly hydrogen-bonded structure, 3, can occur to different degrees for the NO_3^- , PO_3^- , H_2PO_4^- , and RSO_4^- anions but not for the carboxylic



acids which have only two oxygens. It is possible that such electronic differences are responsible for deviations from the correlation in Figure 5 where the nitrate, phosphate, and sulfate hydration energies are seen generally to be relatively larger than

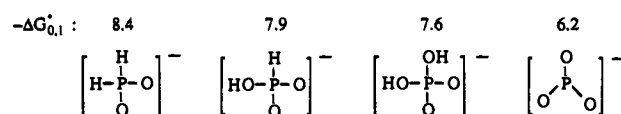
predicted by the straight line correlation which is based mostly on the carboxylic acids.

The importance of the above argument is obscured somewhat when the comparison is made at a free energy, ΔG° , level. Normal frequencies are evaluated for $\text{NO}_3^- \cdot \text{H}_2\text{O}$, structures 1 and 2 are available,²⁷ and the entropy difference between the two structures can be evaluated. The looser structure 2 has a more favorable entropy, and when the $T\Delta S^\circ$ term is included, one finds that the $\Delta G_{0,1}^\circ$ values for the formation of the two structures are essentially the same. Thus, even at room temperature a multiplicity of structures contribute to the stability of the hydrates and the situation becomes less tractable.

A comparison of the $-\Delta G_{0,1}^\circ$ for the sulfonates, Table 1b, with that for the carboxylates, Table 1a, shows that the substituent effects are quite similar. The carboxylate energies decrease in the substituent order $\text{CH}_3 < \text{C}_2\text{H}_5 < \text{CH}_3\text{O} < \text{C}_6\text{H}_5 \ll \text{CF}_3$, while for the sulfonates one observes $\text{CH}_3 < \text{C}_2\text{H}_5 < \text{C}_2\text{H}_5\text{O} \approx \text{C}_6\text{H}_5 \ll \text{CF}_3$. The relative changes for the sulfonates are somewhat smaller corresponding to the smaller absolute magnitude of the $-\Delta G_{0,1}^\circ$ values for these ions.

An examination of the data for all oxo anions in Table 1a,b reveals that the factors leading to stabilization of the oxo-anions and to a decrease of $-\Delta G_{0,1}^\circ$ and also presumably ΔG_{ac}° , can be expressed by a few simple rules: (a) the number of equivalent oxygens over which the negative charge is localized, (b) the presence of electron withdrawing substituents, and (c) the nature and particularly the size of the central atom. The rules will be illustrated by a few examples.

The oxo anions of phosphorus show the following hydration energies (kcal/mol):



The most stabilized anion is PO_3^- which has three equivalent charge delocalizing oxygens. The other three anions have only two such oxygens. The stability differences for these three anions are due to the electron withdrawing substituent effect of the OH group. The stability increases as the number of OH substituents increases from zero to two.

The rule concerning the number of equivalent charge carrying oxygens is followed also by the three groups: NO_2^- , NO_3^- , ClO_2^- , ClO_3^- , ClO_4^- , and IO_3^- , IO_4^- , see Table 1a,b.

When comparing anions with equal number of equivalent charge bearing oxygens and similar substituents but different central atoms such as $\text{C} \leq \text{N} < \text{P} \leq \text{S} \leq \text{Cl} < \text{I}$, one finds that the stability of the anion increases in the above order which is not an order of changing electronegativity but an order of increasing size. Most clear cut examples of this effect are the observed increases of $-\Delta G_{0,1}^\circ$ in the following order: $\text{NO}_3^- < \text{PO}_3^-$ and $\text{ClO}_4^- < \text{IO}_4^-$. On the basis of Table 1a,b and the relationship Figure 5, one expects HIO_4 to be the strongest gas phase acid of all oxo acids whose anions were studied in the present work.

The role of the central atom and its electronic structure could be far more complex. The simple correlation with the size of the atom is a consequence of the dominance of electrostatic effects for the gas phase anions. Large central atoms put the charge bearing oxygens at largest distances from each other. Large atoms are also more polarizable, and this could lead to additional stabilization.

c. Hydration of Singly Charged Anions of Dicarboxylic Acids. The hydration free energies for singly charged anions

(26) Gao, J.; Garner, D. S.; Jorgensen, W. L. *J. Am. Chem. Soc.* **1986**, *108*, 4784.

(27) Shen, M.; Xie, Y.; Schaefer, H. F. *J. Chem. Phys.* **1990**, *93*, 3379.

(28) Ma, B.; Xie, Y.; Shen, M.; Schaefer, H. F. *J. Am. Chem. Soc.* **1993**, *115*, 1943.

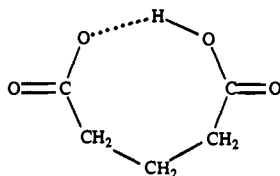
Table 2. Hydration Free Energies of Singly Charge Anions of Dicarboxylic Acids^a

ion	$-\Delta G^{\circ}_{0,1}$	$-\Delta G^{\circ}_{1,2}$
$\text{CO}_2\text{HCO}_2^-$	6.3	
$\text{CO}_2\text{HCH}_2\text{CO}_2^-$	5.3	4.0
$\text{CO}_2\text{H}(\text{CH}_2)_2\text{CO}_2^-$	5.4	~4.0
$\text{CH}_3\text{OCO}(\text{CH}_2)_2\text{CO}_2^-$	8.4	6.1
$\text{CO}_2\text{H}(\text{CH}_2)_3\text{CO}_2^-$	5.5	~4.2
$\text{CO}_2\text{H}(\text{CH}_2)_4\text{CO}_2^-$	5.7	4.4
$\text{CO}_2\text{H}(\text{CH}_2)_5\text{CO}_2^-$	5.5	
$\text{CO}_2\text{H}(\text{CH}_2)_6\text{CO}_2^-$	5.4	
$\text{CO}_2\text{H}(\text{CH}_2)_7\text{CO}_2^-$	5.3	
$\text{CO}_2\text{H}(\text{CH}_2)_8\text{CO}_2^-$	5.0	
1,2 $\text{CO}_2\text{HC}_6\text{H}_4\text{CO}_2^-$	4.7	
1,4 $\text{CO}_2\text{HC}_6\text{H}_4\text{CO}_2^-$	7.4	
<i>cis</i> - $\text{CO}_2\text{HC}_2\text{H}_2\text{CO}_2^-$	5.0	
<i>trans</i> - $\text{CO}_2\text{C}_2\text{H}_2\text{CO}_2^-$	7.3	5.2

^a All values are in kcal/mol. Standard state 1 atm, 293 K.

of dicarboxylic acids are summarized in Table 2. Two classes of compounds were examined, the alkanedioic acids, $\text{HOCO}(\text{CH}_2)_k\text{COOH}$, and the unsaturated systems, 1,2- and 1,4-benzenedicarboxylic acids, and *cis* and *trans* butenedioic acids.

The hydration free energies for the singly charged dicarboxylates with longer alkane links $(\text{CH}_2)_k$, where $k \geq 3$, are found to be quite similar, $-\Delta G^{\circ}_{0,1} \approx 5.3 \pm 0.3$. This value is much lower than the hydration energies of alkylcarboxylates such as propionic acid ($-\Delta G^{\circ}_{0,1} = 9.3$ kcal/mol) Table 1a. The low values for the dicarboxylates are due to the formation of an internal strong hydrogen bond by cyclization of the anion as illustrated below. The hydrogen bond stabilizes the anion and reduces the hydration exothermicity. Cyclization with formation of an internal strong hydrogen bond has been shown



to occur^{29,30} for other bifunctional systems such as the protonated alkane diamines $\text{H}_2\text{N}(\text{CH}_2)_k\text{NH}_3^+$. The evidence was based on the observations^{29,30} that on protonation these systems led to high exothermicities (high $-\Delta H^{\circ}$ values) and considerable losses of entropy (high $-\Delta S$ values) which were consistent with bond formation and loss of freedom due to the cyclization. It was found²⁹ that the rings became strained for $\text{NH}_2(\text{CH}_2)_k\text{NH}_3^+$, with $k < 3$. Thus the cyclization exoergicity, $-\Delta G^{\circ}_{\text{cyc}}$, for $\text{NH}_2\text{CH}_2\text{CH}_2\text{NH}_3^+$ was found to be only ~4 kcal/mol, while that for the higher analogues, up to $k = 6$, was ~12 kcal/mol.^{29,30} The hydration of the cyclized diamines has also been studied,^{11,30} and the exothermicity was found to be low, as expected for an internally hydrogen bonded system.

A comparison of the $-\Delta G^{\circ}_{0,1}$ values for the hydration of the alkane dicarboxylates, and the previous results for the diamines from this laboratory¹¹ is shown in Figure 6. The cyclized dicarboxy compound forms a ring that contains two more chain participating atoms than the diamine with the same number of CH_2 groups. Therefore, the hydration energies for the diamines with k CH_2 groups were plotted at the same x value on the horizontal axis as the hydration energies of the dicarboxylates with $k-2$ CH_2 groups. See below comparison of structures for

(29) Yamdagni, R.; Kebarle, P. *J. Am. Chem. Soc.* **1973**, *95*, 3504.

(30) Meot-Ner, (Mautner) M.; Hamlet, P.; Hunter, E. P.; Field, F. H. *J. Am. Chem. Soc.* **1980**, *102*, 6393.

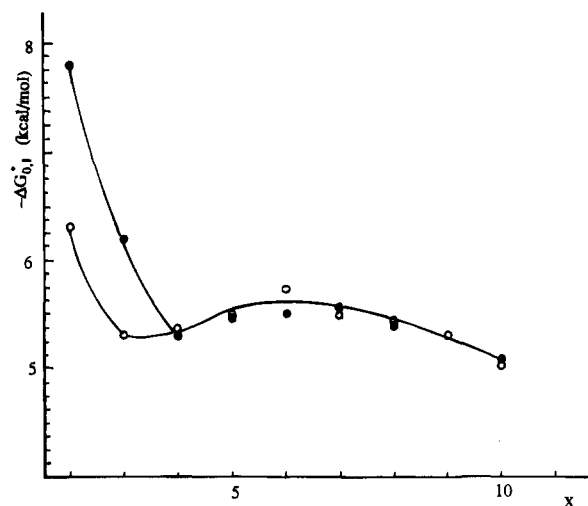
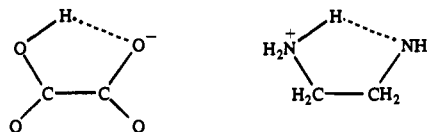


Figure 6. Plot of hydration free energies, $\Delta G^{\circ}_{0,1}$, for the dicarboxylates, $\text{CO}_2\text{H}(\text{CH}_2)_k\text{CO}_2^-$, O, also shown are $\Delta G^{\circ}_{0,1}$ for protonated diamines, $\text{NH}_2(\text{CH}_2)_k\text{NH}_3^+$, ●. Both types of compounds have low $-\Delta G^{\circ}_{0,1}$ values which are due to stabilization of the anions by an internal hydrogen bond which leads to cyclization. The horizontal scale x has been adjusted, $x = k$ (amines); $x = k + 2$ (carboxylates) in order to compare cyclic structure with equal number of atoms in ring. Large increases of $-\Delta G^{\circ}_{0,1}$ for the $x \leq 3$ are due to ring strain which reduces the stabilization of the anion.

$x = 2$. A close correspondence between the two plots is observed for the fairly flat region above $x = 3$, while a sharp



increase occurs below $x = 3$. This increase reflects the decreased stabilization of the anion because of weakening of the internal hydrogen bond due to strain in the ring.

The increase observed for the diamine system is considerably larger. Thus $-\Delta G^{\circ}_{0,1} = 7.8$ kcal/mol for the protonated diamino ethane and only 6.3 kcal/mol for the oxalate ion. This difference probably reflects a larger weakening of the internal hydrogen bond of the diamine relative to the oxalate ion. However also important is the expected low hydration energy of the oxalate ion due to (a) a larger charge delocalization on the anionic carboxylic group (CO_2^-) relative to NH_3^+ and (b) the stabilizing electron withdrawing substituent effect of the neighboring COOH group at the oxalate anion, see structures above. A measure for the significance of factor (a) can be obtained by the difference between the hydration energies for CH_3NH_3^+ ($-\Delta G^{\circ}_{0,1} \approx 11$ kcal/mol)³ and HCO_2^- ($-\Delta G^{\circ}_{0,1} \approx 9$ kcal/mol, Table 1a). The stabilizing substituent effect of the COOH group in the oxalate anion is indicated by the observed difference between the hydration energies, Table 1a, between the acetate ($-\Delta G^{\circ}_{0,1} = 9.4$ kcal/mol) and the cyanoacetate anion ($-\Delta G^{\circ}_{0,1} = 7.1$ kcal/mol). The electron withdrawing effects of CN and CO_2H are known to be of similar magnitude.^{22b}

The flat region of the plot for $x > 3$ shows a low broad maximum centered at $x = 6$. This is observed for both the amino and carboxy systems. The height of the maximum is small and within experimental error, but the feature is probably not an experimental artifact.

The four unsaturated dicarboxylic acids, *cis*- and *trans*- $\text{HCO}_2\text{C}_2\text{H}_2\text{CO}_2\text{H}$ and 1,2- and 1,4- $\text{HCO}_2\text{C}_6\text{H}_4\text{CO}_2\text{H}$, lead to anions whose structures are much more rigid than those of the alkane dicarboxylates. This makes their free energies of

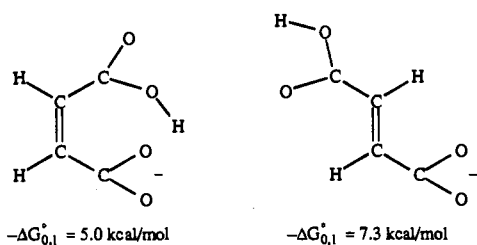
Table 3. Hydration Free Energies of Doubly Charged Anions^a

a. Doubly Charged Ions of Dicarboxylic Acids										
ion		$-\Delta G_{2,3}^{\circ}$		$-\Delta G_{3,4}^{\circ}$		$-\Delta G_{4,5}^{\circ}$		$-\Delta G_{5,6}^{\circ}$		
CO ₂ (CH ₂) ₄ CO ₂ ²⁻		8.4		7.5		6.4		5.8		
CO ₂ (CH ₂) ₅ CO ₂ ²⁻		8.0		7.2		6.2		5.5		
CO ₂ (CH ₂) ₆ CO ₂ ²⁻		7.8		7.1		6.1		5.5		
CO ₂ (CH ₂) ₇ CO ₂ ²⁻		7.6		6.9		5.9		5.2		
CO ₂ (CH ₂) ₈ CO ₂ ²⁻		7.4		6.7		5.8		5.1		
1,4 CO ₂ C ₆ H ₄ CO ₂ ²⁻		8.4		7.3		6.3		5.9		

b. Doubly Charged Anions of Some Oxo Acids of Sulfur and Selenium										
ion	$(n-1,n)$ and $-\Delta G_{n-1,n}^{\circ}$ (kcal/mol)									
sulfate SO ₄ ²⁻	(5,6)	8.5	(6,7)	7.5	(7,8)	6.7	(8,9)	6.0	(9,10)	5.5
	(10,1)	5.0								
selenate SeO ₄ ²⁻	(5,6)	8.0	(6,7)	7.0	(7,8)	6.3	(8,9)	5.6		
thiosulfate S ₂ O ₃ ²⁻	(4,5)	8.3	(5,6)	7.3	(6,7)	6.5	(7,8)	5.9	(8,9)	5.3
	(9,10)	4.7								
dithionate O ₃ SSO ₃ ²⁻	(2,3)	9.4	(3,4)	8.0	(4,5)	7.1	(5,6)	6.3	(6,7)	5.6
	(7,8)	5.1								
ethane disulfonate SO ₃ C ₂ H ₄ SO ₃ ²⁻	(1,2)	8.7	(2,3)	7.5	(3,4)	6.6	(4,5)	5.9	(5,6)	5.3
persulfate O ₃ SOOSO ₃ ²⁻	(1,2)	8.5	(2,3)	7.5	(3,4)	6.7	(4,5)	5.9	(5,6)	5.4
tetrathionate O ₃ SSSSO ₃ ²⁻	(0,1)	9.1	(1,2)	7.8	(2,3)	6.7	(3,4)	6.1	(4,5)	5.4
1,5 naphthalene-disulfonate	(0,1)	7.8	(1,2)	7.0	(2,3)	6.3	(3,4)	5.5		

^a All values are in kcal/mol. Standard state 1 atm, 293 K.

hydration of special interest. The $-\Delta G_{0,1}^{\circ}$ for the *cis*- and *trans*-dicarboxyethylene are given below.



The energy value for the *trans* isomer is similar to values observed for anions stabilized by electron withdrawing substituents, see for example difluoroacetate (7.5 kcal/mol). The *trans* anion is stabilized by both the vinyl group³² and the COOH substituent. The much lower value for the *cis* isomer indicates additional stabilization of the anion by internal hydrogen bond formation. Space filling models of the maleate anion indicate that the carboxylic groups are very crowded. The anion is not planar because the carboxylic groups have rotated around the C-C bonds to release strain. The internal H bond in this ion is probably more strained than the bond in the much less rigid CO₂H(CH₂)₂CO₂⁻ anion.

The hydration free energies for the 1,4- and 1,2-benzenedicarboxylates, Table 2, are similar to those discussed above and the effects for these compounds are also expected to be similar. These data provide a confirmation for the consistency of the experimental results.

d. Hydration Energies of Doubly Charged Anions. The hydration energies of doubly charged anions determined in this work are given in Table 3. The values obtained are also shown in Figure 7, where the $-\Delta G_{n-1,n}^{\circ}$ are plotted versus n . The data are based on those equilibrium constants $K_{n-1,n}$ which could be determined at room temperature when the H₂O partial pressure was in the range 1 to ~50 mTorr. For very strongly hydrating species only the higher $n-1,n$ equilibria were

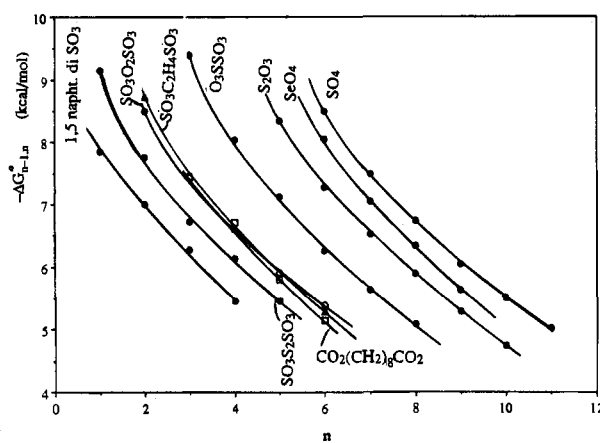


Figure 7. Hydration free energies $\Delta G_{n-1,n}^{\circ}$ for several doubly charged anions. Hydration exothermicity increases in the following order: 1,5 di SO₃ naphthalene²⁻, SO₃S₂SO₃²⁻, SO₃O₂SO₃²⁻, SO₃C₂H₄SO₃²⁻, CO₂(CH₂)₆CO₂²⁻, SO₃SO₃²⁻, S₂O₃²⁻ (thiosulfate), SeO₄²⁻, SO₄²⁻. These results reflect the stabilization on the anions with increasing distance between the two charged groups.

observed, while the determinations for a more weakly hydrating species could be obtained at lower $n-1,n$ including (0,1) for the weakest hydrating species. Examination of the plots for the individual anions from left to right, *i.e.*, from low to high n reveals at a glance the order of increasing hydration strength: 1,5-naphthalenedisulfonate, tetrathionate O₃SSSSO₃²⁻, persulfate, O₃SOOSO₃²⁻, 1,2-ethanedisulfonate SO₃CH₂CH₂SO₃²⁻, alkanedicarboxylates CO₂(CH₂)_kCO₂²⁻ $k = 4-8$, dithionate, O₃SSO₃²⁻, thiosulfate SO₃S²⁻, selenate SeO₄²⁻, sulfate SO₄²⁻.

The slope for each plot shows an increase as n is decreased. The values of n at which rapid increases of the slope occur, follow the same order as above. Thus, the rapid increase occurs at $n \approx 1$ for 1,5-naphthalenedisulfonate and at $n \approx 6$ for the sulfate anion.

The order observed in the plots is easily rationalized. First we shall consider the cases where two functional groups are

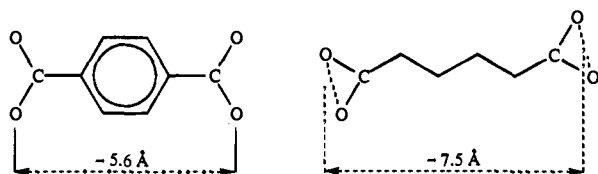
present leading to two distinct charge centers. The doubly charged anions like SeO_4^{2-} , $\text{S}_2\text{O}_3^{2-}$ (thiosulfate), and SO_4^{2-} could then be considered as special cases where the distance between the two charge centers is very small. Two major factors determine the observed order of hydration energies: (a) The distance between the two charged groups. This most important factor is a consequence of the intense coulombic repulsion between the two charges which is present in the gas phase. (b) The charge delocalization within the functional group, *i.e.*, $-\text{SO}_3^- > -\text{CO}_2^-$. The order of stabilization by charge delocalization was examined in the preceding section dealing with monobasic group anions. It was established that the stabilization increases with the number of equivalent oxygens over which the charge is delocalized and with the size of the central atom. A large central atom leads to stabilization because it increases the distance between the negative oxygens.

Examples illustrating (a) and (b) will be given: (a) The importance of distance between the charges is most clearly demonstrated by the observed increase of hydration exothermicities of the dicarboxylates $\text{CO}_2(\text{CH}_2)_k\text{CO}_2^{2-}$ with decreasing k . This series will be examined later in greater detail. However the increase in the order $\text{SO}_3\text{S}_2\text{SO}_3^{2-}$, $\text{SO}_3\text{O}_2\text{SO}_3^{2-}$, $\text{SO}_3\text{-CH}_2\text{CH}_2\text{SO}_3^{2-}$, $\text{O}_3\text{SSSO}_3^{2-}$ is also mainly determined by the decreasing distance between the two charged $-\text{SO}_3^-$ groups.

(b) The effect of the nature of the charge delocalization within each functional group is well illustrated by the observed substantial increase of hydration energy from $\text{SO}_3\text{CH}_2\text{CH}_2\text{SO}_3^{2-}$ to $\text{CO}_2\text{CH}_2\text{CH}_2\text{CO}_2^{2-}$. The results in Figure 7 show that the hydration energies of the dicarboxylates become the same as that for the ethanedisulfonate only after the carboxylate chain increases to $k = 8$, an impressive difference.

A third factor due to the stabilizing effect of charge delocalization from the functional group to the moiety connecting the two groups might be expected also. Different moieties connecting two charged groups separated by the same distance could be expected to lead to differing hydration energies due to the differential stabilization that might be provided by these moieties.

Clear cut evidence for such an effect does seem to be available in the present results. This can be shown by considering one example: a comparison of the hydration of 1,4- $\text{CO}_2\text{C}_6\text{H}_4\text{CO}_2^{2-}$ ($-\Delta G_{2,3}^\circ = 8.4$ kcal/mol) and $\text{CO}_2(\text{CH}_2)_4\text{CO}_2^{2-}$ ($-\Delta G_{2,3}^\circ = 8.4$ kcal/mol) whose structures are shown below.



Also shown are the estimated (33) distances between the two charge centers. An estimate of the increase of $-\Delta G_{2,3}^\circ$ for a hypothetical alkanedioate dianion with a charge separation equal to that of the benzenedicarboxylate dianion, 5.6 Å, can be obtained from an extrapolation of the $-\Delta G_{2,3}^\circ$ data for these acids as a function of k and thus the separation (34). The estimated increase is 0.8 kcal/mol, giving a $-\Delta G_{2,3}^\circ = 8.4 + 0.8 = 9.2$ kcal/mol. The 0.8 kcal/mol between this value and the 8.4 kcal/mol for 1,4-benzenedicarboxylate dianion is attributed to a larger stabilization of this anion relative to the alkanedioate of the same charge separation due to the delocalization and polarization of the electrons in the aryl moiety. Although this dianion has two distinct charge centers, the charges are not totally isolated. Hydration of one charge center causes a redistribution of the π electrons resulting in a partial

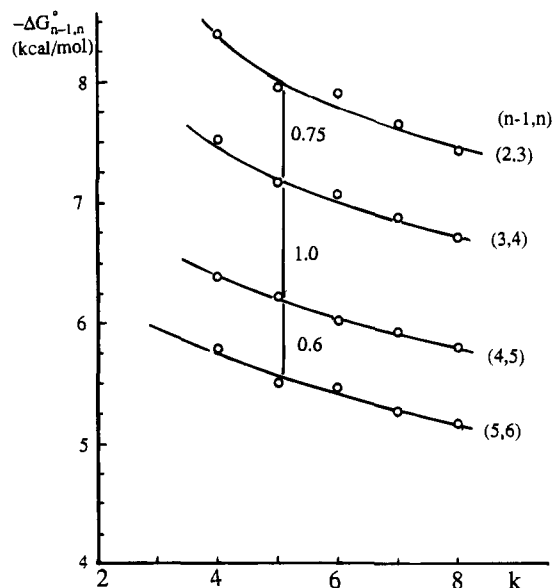


Figure 8. Hydration free energies $\Delta G_{n-1,n}^\circ$ for doubly charged dicarboxylates, $\text{CO}_2(\text{CH}_2)_k\text{CO}_4^{2-}$, with increasing chain length.

stabilization of the second charge center. The $-\Delta G_{0,1}^\circ$ value would be a more sensitive probe of this stabilization, and these values will be available when equilibrium measurements are extended to higher temperatures.

The plots of the $-\Delta G_{n-1,n}^\circ$ values in Figure 7 are fitted to smooth curves. Actually, discontinuous changes of the values as a function of n can be expected since the stabilities of the hydrates depend on the specific structures of the individual hydrates. The fact that the data can be approximately fitted to smooth curves indicates that specific structural features do not have a large effect on the hydration energies. A more detailed examination of the energy values for the alkanedicarboxylates shows that some structural effects can be found.

A plot of the $-\Delta G_{n-1,n}^\circ$ of the dicarboxylates $\text{CO}_2(\text{CH}_2)_k\text{CO}_2^{2-}$ is shown in Figure 8. In each plot the $-\Delta G_{n-1,n}^\circ$ at constant n are plotted against the value of k . Comparing the four plots one finds that the energy difference between them does not decrease regularly as n is increased. The observed difference $(-\Delta G_{2,3}^\circ) - (-\Delta G_{3,4}^\circ) = \Delta\Delta G_4^\circ \approx 0.8$ kcal/mol is smaller than $\Delta\Delta G_5^\circ \approx 1.0$ kcal/mol which is followed by the smallest $\Delta\Delta G_6^\circ \approx 0.6$ kcal/mol. A similar pattern was observed in earlier work^{10,11} for the hydration of the doubly charged diamines, $\text{NH}_3^+(\text{CH}_2)_k\text{NH}_3^+$. The cause should be the same. When two separated charge centers are present, successive incoming water molecules will alternate between the two centers, the first going to either charge center, the second to the other. The third molecule will have to double up with one of the water molecules. Such doubling up leads to a larger drop of hydration energy. The fourth molecule will double up on the other charge center, and the $\Delta\Delta G_4$ will be relatively low. The fifth water molecule will have to triple up leading to a relatively large $\Delta\Delta G_5$, while the sixth molecule also tripling up will lead to a relatively low $\Delta\Delta G_6$, as observed in Figure 8. Ions without a distinct separation of charges, such as SO_4^{2-} , SeO_4^{2-} , etc., Table 3b, do not follow the same pattern, showing constantly decreasing $\Delta\Delta G$ values.

(31) The monocarboxylic acid, $\text{CH}_2\text{CHCO}_2\text{H}$ is more acidic by some 1 kcal/mol than formic acid.³²

(32) Graul, S. T.; Schnute, M. E.; Squires, R. R. *J. Mass Spectrom. and Ion Proc.* **1990**, *96*, 181.

(33) Estimate of distances based on $\text{C}=\text{C}$ aromatic 1.399 Å. $\text{C}-\text{CO}_2$ 1.5 Å, $\text{C}=\text{O}$ 1.4 Å and $\text{C}-\text{C}$ 1.54 Å.

e. Enthalpy Changes and Temperature Dependence of Equilibria. The present apparatus operates only at room temperature, and therefore the results provide only equilibrium constants and free energy changes at ~ 300 K. Approximate $\Delta H^\circ_{n-1,n}$ values can be obtained for the singly charged, not cyclized ions from the present $\Delta G^\circ_{n-1,n}$ by subtracting 7 kcal/mol from the $\Delta G^\circ_{n-1,n}$ value. The ΔS value for the $n-1,n$ reactions is often ~ 24 cal/degree mol³, and this leads to a $T\Delta S$

(34) The estimate was obtained by extrapolating the $-\Delta G^\circ_{2,3}$ value to $k = 2$ using $\Delta G^\circ_{2,3}$ values for $k = 4$ and 6. This led to $\Delta G^\circ_{2,3}$ ($k = 4$) $-\Delta G^\circ_{2,3}$ ($k = 2$) ≈ 1 kcal/mol. This difference was then divided by the distance difference for $k = 2-4$ (~ 2.5 Å) and multiplied by the 1.9 Å difference between the hexanedioate and 1,4-benzenedicarboxylate charge centers.

term of ~ 7 kcal/mol. For the doubly charged ions the loss of freedom will be larger, and a value of -8 or -9 kcal/mol might be more appropriate.

A variable temperature ion source using the same design as shown in Figure 1 which will lead to equilibrium determinations over a wide temperature range and to ΔH° and ΔS° determinations has just been developed and put into operation.

Acknowledgment. This work was supported by grants from the Canadian Natural Sciences and Engineering Research Council (NSERC).

JA951796I